GEOPHYSICS, VOL. 63, NO. 4 (JULY-AUGUST 1998); P. 1310–1317, 8 FIGS.

Seismic reflection and ground-penetrating radar imaging of a shallow aquifer

Steven J. Cardimona*, William P. Clement‡, and Katharine Kadinsky-Cade**

ABSTRACT

In 1995 and 1996, researchers associated with the US Air Force's Phillips and Armstrong Laboratories took part in an extensive geophysical site characterization of the Groundwater Remediation Field Laboratory located at Dover Air Force Base, Dover, Delaware. This field experiment offered an opportunity to compare shallow-reflection profiling using seismic compressional sources and low-frequency ground-penetrating radar to image a shallow, unconfined aquifer. The main target within the aquifer was the sand-clay interface defining the top of the underlying aquitard at 10 to 14 m depth. Although the water table in a well near the site was 8 m deep, cone penetration geotechnical data taken across the field do not reveal a distinct water table. Instead, cone penetration tests show a gradual change in electrical properties that we interpret as a thick zone of partial saturation. Comparing the seismic and radar data and using the geotechnical data as ground truth, we have associated the deepest coherent event in both reflection data sets with the sand-clay aquitard boundary. Cone penetrometer data show the presence of a thin lens of clays and silts at about 4 m depth in the north part of the field. This shallow clay is not imaged clearly in the low-frequency radar profiles. However, the seismic data do image the clay lens. Cone penetrometer data detail a clear change in the soil classification related to the underlying clay aquitard at the same position where the nonintrusive geophysical measurements show a change in image character. Corresponding features in the seismic and radar images are similar along profiles from common survey lines, and results of joint interpretation are consistent with information from geotechnical data across the site.

INTRODUCTION

The Groundwater Remediation Field Laboratory (GRFL), located on Dover Air Force Base, Dover, Delaware, consists of an unconfined aquifer extending down to 14 m depth. The surface of the site is a 3.5-acre grass-covered field with a gentle slope to the east and only minor topographic undulations of less than 0.5 m. We present a portion of geophysical and geotechnical site characterization data collected at the GRFL in 1995 and 1996 (Figure 1) that relates to the comparison of seismic and ground-penetrating radar (GPR) reflection profiling results. The goal of our experiment was to image the aquitard boundary at 10 to 14 m depth (dipping toward the north) with both reflection methods. Because the GRFL was thought to be a sandy, fresh-water aquifer with a shallow water table, we anticipated both seismic and GPR methods would be successful. Geotechnical work, however, revealed a more heterogeous aquifer than expected, including a clay lens at about 4 m depth discovered in the north end of the field (Figure 2). This thin, 1 to 2-m-thick shallow lens of clays and silts in the north changes abruptly at 80 to 90 m north to a wider 3 to 4-m-thick silty sand lens in the south. Also, the water table as measured in a monitoring well at the site was at 8 m depth instead of about 3 m as expected from prior (mis)information.

To image the upper 15 m of the subsurface with seismic reflection methods is challenging. Generating and transmitting high frequencies is necessary to image such shallow depths. Slow near-surface velocities help increase potential resolution. Because the water table and the aquitard boundary are so close together, our recorded seismic data cannot resolve separate reflections from these two features. The recorded image would be the result of interference between energy reflected from both

Presented at the 66th Annual International Meeting, Society of Exploration Geophysicists, as Coincident ground-penetrating radar and seismic imaging of an aquitard boundary. Manuscript received by the Editor April 17, 1997; revised manuscript received September 26, 1997.
*University of Missouri–Rolla, Rolla, Missouri 65409-0410. E-mail: cardi@umr.edu.
‡Boston College, 29 Randolph Road, Hanscom AFB, MA 01731-3010. E-mail: billc@doc.plh.af.mil.
**Air Force Phillips Laboratory, 29 Randolph Road, Hanscom AFB, MA 01731-3010. E-mail: kadinsky@terra.plh.af.mil.

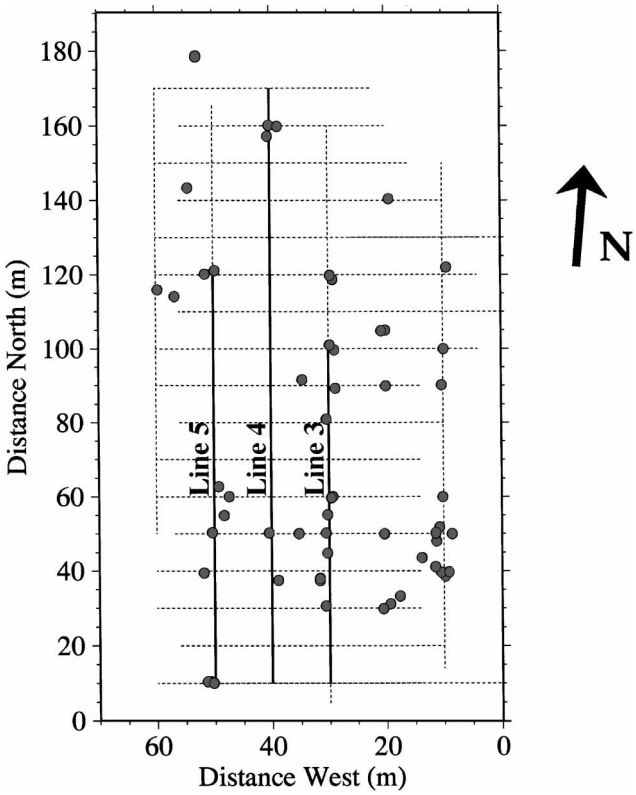

FIG. 1. Site map of geophysical survey layout at the GRFL. Lines 3–5 are seismic reflection profiles: (3) firing rod, (4) sledgehammer, (5) vibrator. Dashed lines show GPR survey grid. Dots across the field show cone penetrometer test points.

geologic features. However, cone penetration test (CPT) data (Figure 3) show that a sharp water table boundary does not exist. Where there is a transition, CPT measurements change gradually in a zone at least 1 m thick. We interpret the geotechnical data to indicate a thick zone of increasing partial saturation. Thus, the water table does not reflect much elastic energy, and the seismic data are able to image the aquitard boundary without interference from a water table event.

As the water saturation of a soil increases, the seismic velocity increases and the corresponding resolution decreases. On the other hand, GPR resolution improves as soil saturation

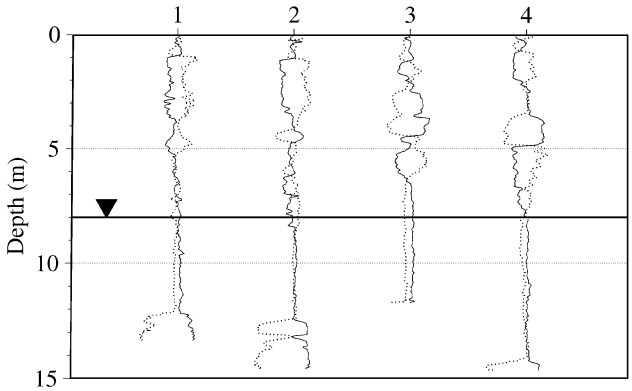

FIG. 3. Cone penetration dielectric (solid line) and resistivity (dotted line) logs from four locations across the GRFL. The water table marked at 8 m was measured in the monitoring well at the site. There is no abrupt change in electrical properties of the soil, indicative of a sharp water table.

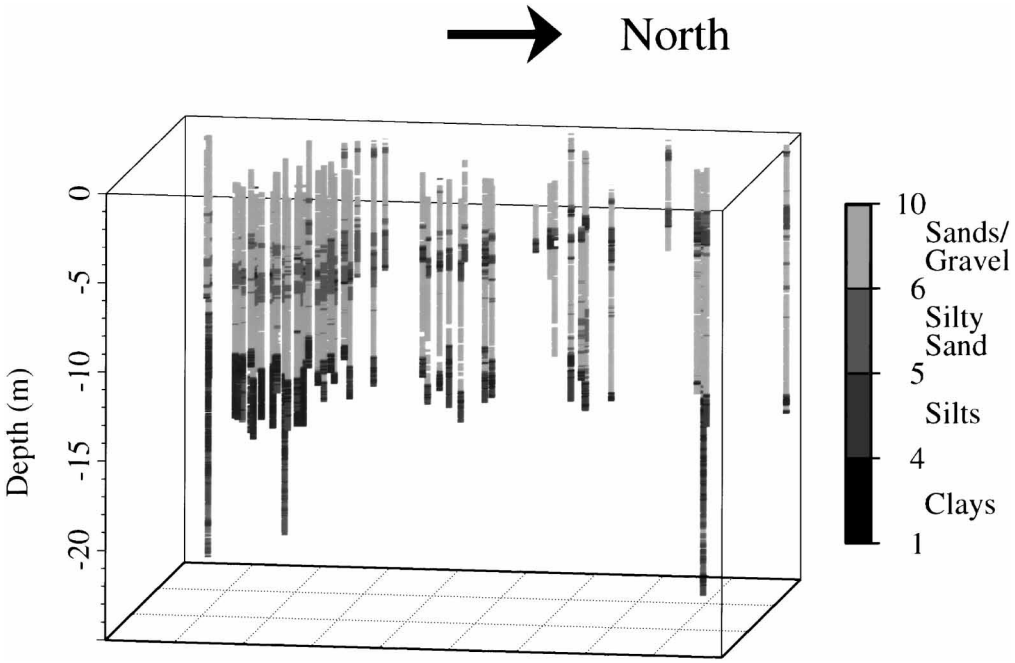

FIG. 2. Soil classification data from cone penetrometer measurements. Classifications are grouped into four primary units: sands/gravels, silty sand, silts, and clays. The change from south to north within the aquifer (from silty sand to lens of silts/clays) and in the aquitard (from clays to silts) occurs around 80 to 90 m north.

increases because radar velocities decrease. The change in velocity below the water table is greater for the seismic data than the GPR because the electromagnetic wave velocity changes only as the square root of the dielectric constant. Even though we recorded a variety of radar frequencies, we compare the low-frequency radar with the seismic data because they have similar wavelengths and because corresponding vertical and horizontal resolution are comparable. For example, a seismic velocity of 475 m/s for 100-Hz seismic signals in the unsaturated zone (from near-surface refraction) and a radar velocity of 0.1 m/ns for 20-MHz radar signals (average velocity across the field) yield data with a common wavelength of 4 to 5 m. The comparison of reflection images over common survey lines shows many similar features between the low-frequency radar and the seismic data.

The CPT geotechnical data acquired at the GRFL provide geological characterization of the subsurface to compare with the images obtained from the geophysical data. Applied Research Associates Inc. operated a cone penetrometer to measure in-situ physical properties. The geotechnical data include soil classification (Figure 2) based on sleeve and tip stress ratios (Robertson, 1990) and measurements of resistivity and dielectric constant of the soils (Figure 3). We use the aquitard boundary at 10–14 m as a reference to compare the geophysical reflection data. Despite the lateral heterogeneity within the aquifer and the deeper-than-expected water table, the GRFL data offer a unique comparison of seismic and GPR profiles at a field site where there is substantial geotechnical sampling.

METHODS

Seismic surveys

We acquired seismic data along three north–south profiles set 10 m apart in the east–west direction. Because a separate goal of our experiment was to compare seismic sources (Cardimona et al., 1996b), we used a different compressional source for each seismic profile: a 5.5-kg sledgehammer, a 12-gauge firing rod (buffalo gun) from Betsy Seisgun Inc., and the Earth Reaction Seismic Source (ERSS), a portable piezoelectric vibrator developed by Elohi Geophysics. We collected 24-channel common-midpoint (CMP) data with 100-Hz vertical geophones, shooting end-on with a 1-m offset between source and nearest geophone and a common shot and receiver spacing of 0.5 m for all lines. The CMP bin interval was 0.25 m, resulting in 12-fold data. We chose our acquisition parameters to image the very shallow structure at the GRFL.

With the sledgehammer source, we collected 320 shot gathers along a line through the central portion of the field (line 4, Figure 1). Source repeatability was not consistent because of different sledgehammer operators and the length of day in the field. However, stacking eight blows per shotpoint adequately equalized source wavelet and signal strength, based on a qualitative assessment of recorded shot gathers during acquisition. Figure 4a shows a representative shot gather from the sledgehammer survey prior to filtering. A slow direct wave (250 m/s) overlaps with the ground roll at near offsets. A shallow refractor at about 1 m depth with a velocity of 475 m/s is strong in the far offset traces.

Ten meters to the east of the sledgehammer line, we collected 180 shot gathers with the 12-gauge firing rod (line 3, Figure 1), shooting 150-grain blanks. Holes were drilled about 1 m deep, and the CMP data were collected with dirt-tamped holes to enhance source coupling. Figure 4b shows a representative shot gather. Whereas the sledgehammer had a large ratio of ground-roll to body-wave energy, the firing rod's strongest arrival is the 475-m/s refraction event that is more prominent than the airwave on some records.

Ten meters to the west of the sledgehammer line, we collected 220 shot gathers using the ERSS vibrator (line 5, Figure 1). We operated the ERSS with a linear, 3-s sweep of 90 to 450 Hz, and we stacked eight sweeps at each source point. We recorded uncorrelated data and later crosscorrelated the data with a synthetic sweep. Although the vibrator records (e.g., Figure 4c) do not show strong first arrivals, the ground-roll and airwave energy relative to body-wave energy is considerably less than with either impulsive source.

The data from each different source were processed with similar steps. First, we applied a zero-phase, 80–300-Hz band-pass filter with 18-dB/octave high- and low-cut roll off. Then we used a frequency-wavenumber (f-k) filter to remove airwave and ground-roll energy and a mute to remove the shallow refraction (compare with Figures 4b and 4d). Both the first-arrival mute and the f-k operator had 5-ms taper length. The f-k filtering introduced some reverse-slope artifacts in the shot gathers, but CMP stacking reduced this noise. We used constant-velocity stacks to determine the normal moveout (NMO) velocity. Corrections for elevation were unnecessary because of the minor effect on stack quality, but we did apply some corrections to the firing rod data to compensate for variations in shot trigger times.

For signal enhancement and to give a horizontal trace interval equal to 1 trace/m for comparison with the GPR, we summed four adjacent CMP stacked traces before plotting. This horizontal sample rate of 1 trace/m is smaller than the Fresnel zone for our data, so spatial aliasing is not a concern. We used a 50-ms automatic gain control (AGC) window for display only.

Radar surveys

The University of Delaware deployed the bistatic Sensors and Software pulseEKKO IV (PEIV) GPR system with 25-MHz antennae for reconnaissance of the field at discrete 1-m reflection points along a 10×10 m grid. Three of the north–south GPR survey lines coincide with the seismic profiles (Figure 1). The PEIV was operated with a 1000-V transmitter and a 4-m antennae separation. Total recording time was 600 ns with a 2.4-ns sample interval. Each trace was a stack of 128 scans. We used CMP data from the PEIV for radar velocity analysis. We also applied time-zero adjustments and amplitude debias corrections and used an AGC window of 125 ns for display.

Hager Geoscience Inc. used the monostatic Subsurface Interface Radar (SIR-2) of Geophysical Survey Systems Inc. to collect continuous GPR with 20-MHz antennas over the same 10×10-m grid as with the PEIV (Figure 1). The recording time was 900 ns, and the number of samples per trace was 1024. The monostatic radar system operated at 16 scans/s, and the data-collection fold was 16. The average collection rate was about 45 traces/m. The SIR-2 unit applied a predefined, nonlinear gain to the data. Data processing for the continuous GPR included subtraction of the average trace to reduce

first-arrival energy and antenna ringing and time-zero adjustment. We stacked multiple traces of the SIR-2 data to increase the nominal fold and to make the horizontal sampling equal to that of the PEIV data. As with the seismic data, this horizontal sample rate of 1 trace/m does not introduce spatial aliasing. An AGC window of 175 ns was used for display.

RESULTS

Figures 5–7 display the stacked seismic sections (Figure 5: line 3, firing rod; Figure 6: line 4, sledgehammer; Figure 7: line 5, vibrator) and the profiles from the two radar sources for the three different survey lines. We pick events in the firing rod, sledgehammer, and GPR profiles at the onset of the reflection wavelets. After crosscorrelation, however, the vibrator data are nominally zero phase, and events correspond to the peak in the reflection wavelets. The seismic event at ~42 ms (e.g., Figure 5, south end) and the 225-ns reflection (e.g., Figure 5, south end) in the radar profiles correspond to a depth of ~12 m. Seismic refraction data indicate a velocity increase at a depth of 8 m (Clement et al., 1997), corresponding to the water table in the monitoring well at the GRFL. However, high-frequency (50, 100, and 200 MHz) PEIV radar profiles do not record a water table reflection across the survey area (Clement et al., 1997). Also, CPT measurements of resistivity and dielectric constant (Figure 3) do not show an abrupt change in properties at the water table. Increasing water saturation over a thick zone would explain the absence of a water table event in the GPR and

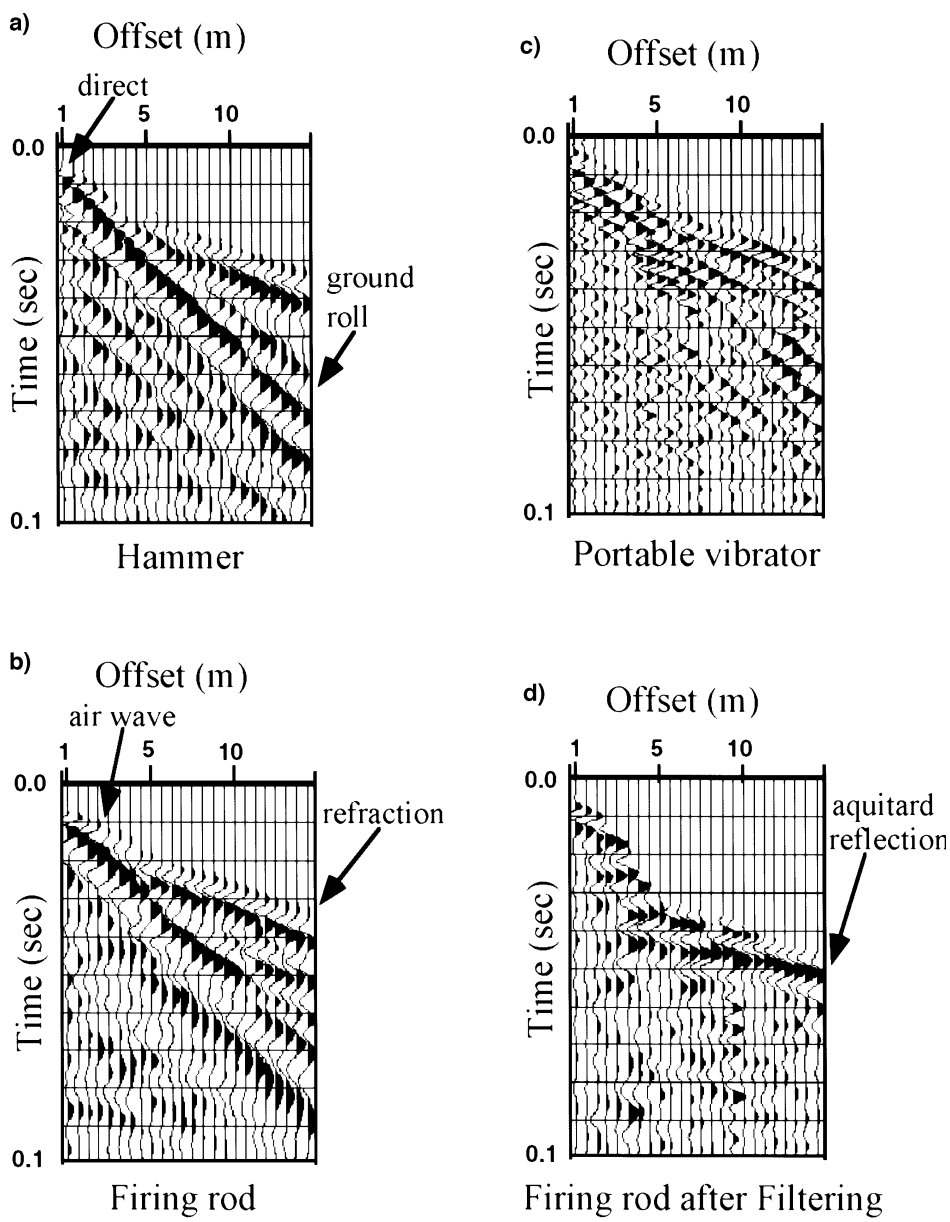

FIG. 4. Shot records with 50-ms AGC for display: (a) sledgehammer gather, (b) firing rod gather, (c) portable vibrator gather (after 80 to 300-Hz band-pass filter), (d) firing rod gather of (b) after 80- to 300-Hz band-pass filter, f-k filter, and mute. The reflection from the aquitard is clear in (d).

seismic reflection data. We interpret the event corresponding to 12 m depth in Figures 5–7 as a reflection from the aquitard boundary.

Previous work in coastal plain sedimentary environments similar to the GRFL (Miller et al., 1986) suggests that compressional sources should generate adequate energy for seismic reflection data acquisition. In Figures 5–7, the aquitard is imaged with all three seismic sources. Visual assessment of the records shows that the firing rod source has the best signal-to-noise (S/N) ratio and the best lateral continuity of the aquitard reflection event. The firing rod data maintain a strong and fairly constant source amplitude, the vibrator source has the broadest bandwidth signal, and the sledgehammer offers a source strength that lies between those of the firing rod and the vibrator, with by far the most rapid data collection rate of the three sources.

In the GPR data, we chose the longer AGC window for the SIR-2 data compared with that of the PEIV (175 ns versus 125 ns) to compensate for the apparent lower S/N ratio in the continuous-recording GPR. Light poles to the east in the north side of the field and a fence corner to the southwest introduce airwave diffractions and limited interference in all the radar profiles (Figures 5–7).

The sand-clay interface at ~12 m represents an impedance contrast for both electromagnetic and elastic waves, and the GPR and seismic reflection data image the aquitard boundary clearly (Cardimona et al., 1996a). The seismic data show that the reflection from the aquitard boundary arrives earlier in the north than in the south. This time difference is offset by increasing stacking velocities from ~450 m/s in the south to ~700 m/s in the north, resulting in an aquitard boundary that is deeper in the north than in the south. The radar velocity variation is less systematic than the seismic velocity variation, showing no consistent trend across the GRFL site. The depth to the aquitard boundary interpreted from the radar sections correlates with CPT measurements, indicating the aquitard increases in depth from 10.5 m in the south to 14.5 m in the north. The time-to-depth conversion using stacking velocities for the aquitard reflection in the seismic profiles correlates with the depth to the aquitard in the GPR and CPT data.

The reflection from the aquitard disappears in both radar data sets and in the seismic reflection profiles north of 90 m. In the radar data, the shallow clay layer in the north (Figure 2) may conductively attenuate the radar signal. Alternatively, diffractions from above-ground obstacles to the northeast (see Figures 5–7) could interfere with the aquitard reflection event. These mechanisms could explain the loss of the sand-clay reflection in the north portion of the GPR profiles. However, the seismic data exhibit a similar change in image quality of the aquitard boundary reflection. CPT data reveal a change in soil classification within the aquitard, from clay in the south to silt in the north (Figure 2). We interpret that the changes

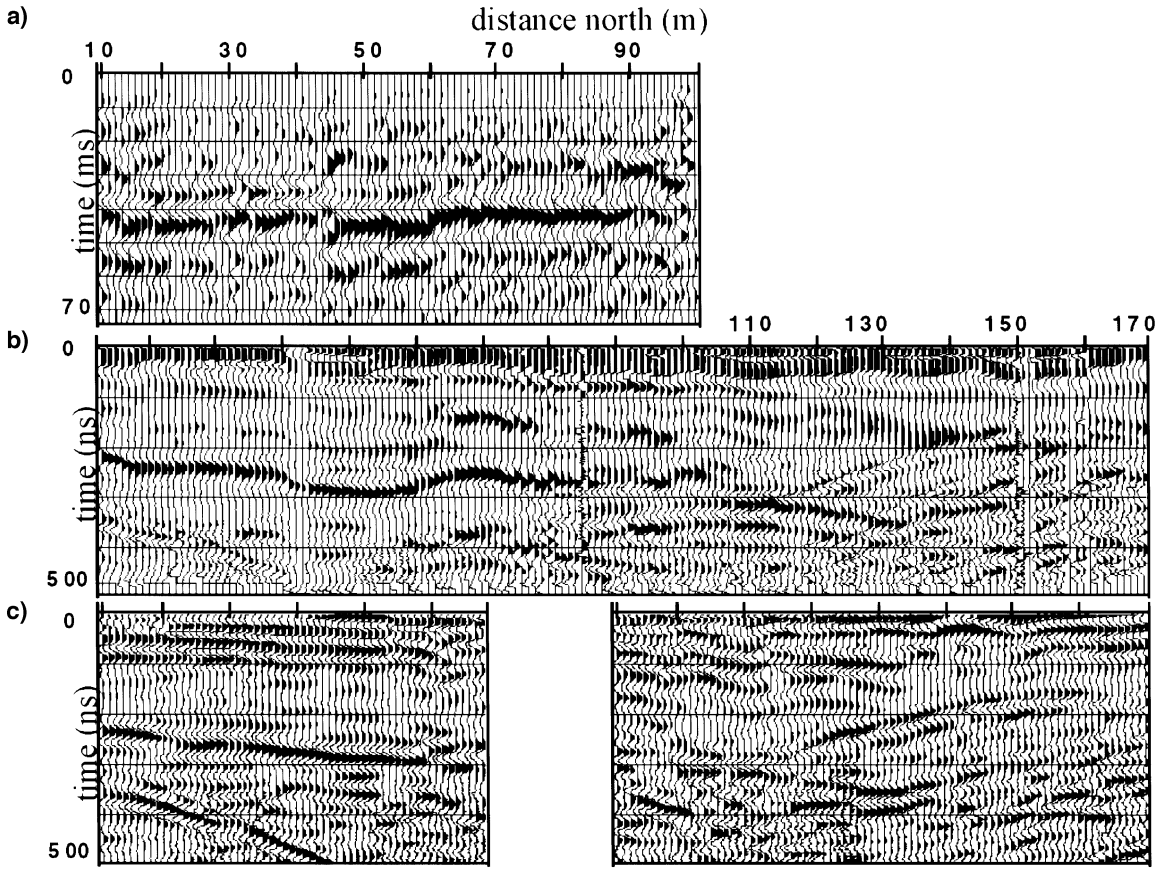

FIG. 5. Reflection records for line 3: (a) firing rod, (b) PEIV radar, (c) SIR-2 radar. The reflection event at 42 ms (south end) in the seismic data and at 225 ns (south end) in the radar data corresponds to the aquitard boundary. The seismic event at ~25 ms north of 90 m corresponds to the shallow lens of silts and clays.

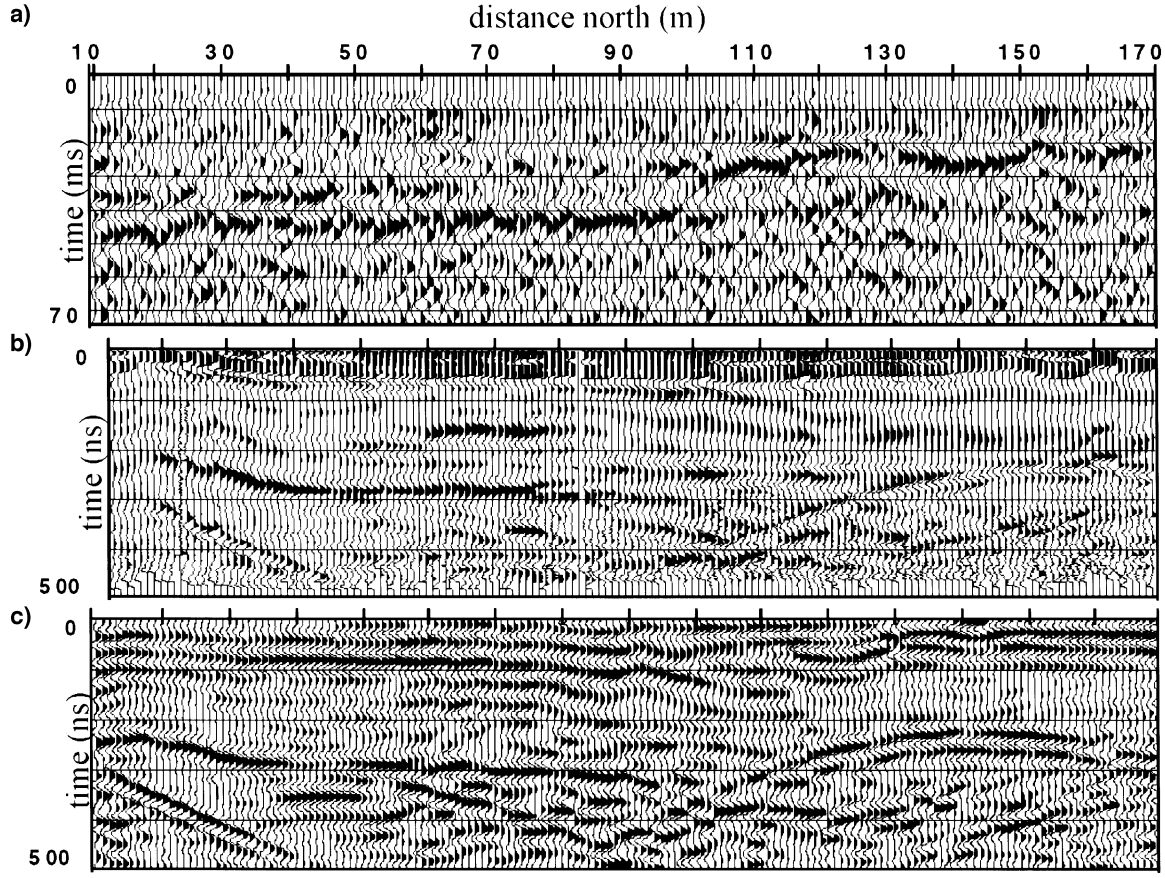

FIG. 6. Reflection records for line 4: (a) sledgehammer, (b) PEIV radar, (c) SIR-2 radar. The reflection event at 42 ms (south end) in the seismic data and at 200 to 250 ns in the radar data corresponds to the aquitard boundary. The seismic event at ~25 ms north of 95 m corresponds to the shallow lens of silts and clays.

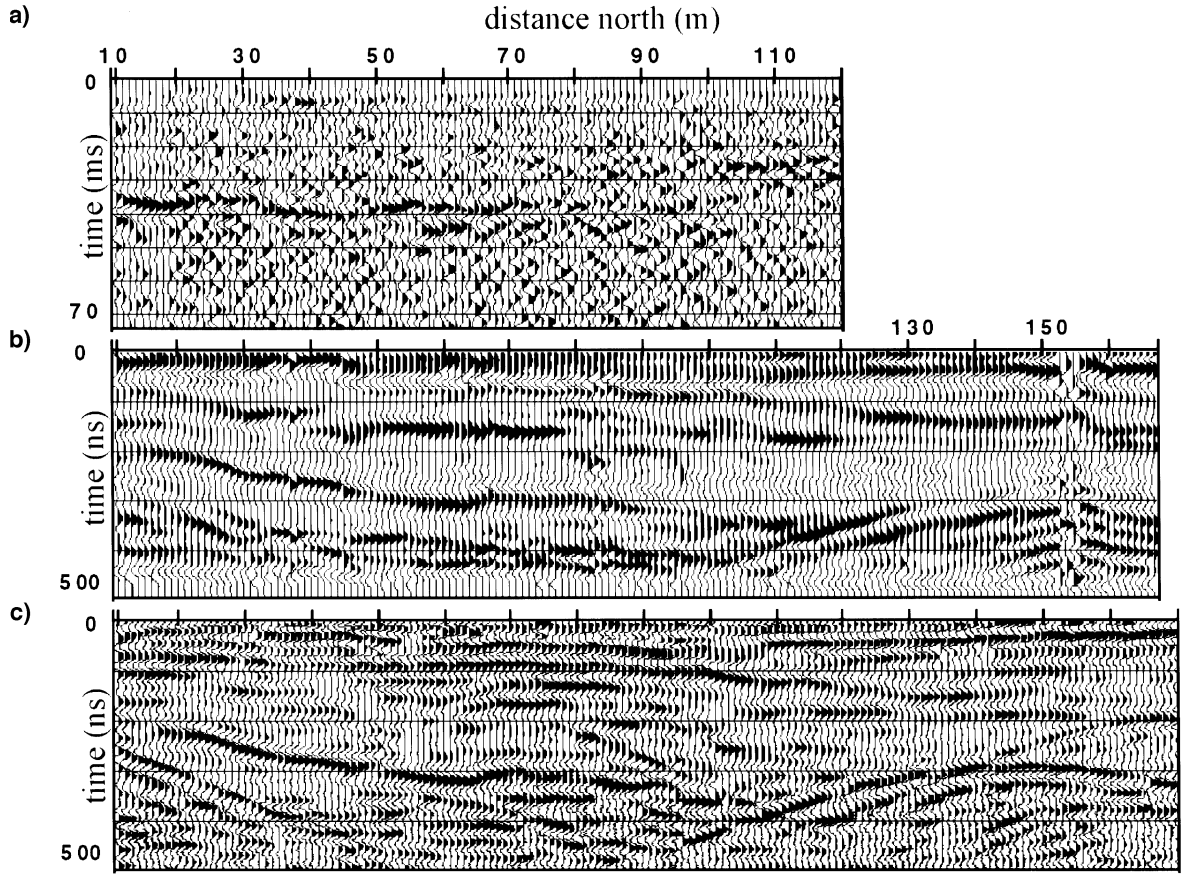

FIG. 7. Reflection records for line 5: (a) portable vibrator, (b) PEIV radar, (c) SIR-2 radar. The reflection event at 38 to 40 ms in the seismic data and at 190 to 275 ns in the radar data corresponds to the aquitard boundary. The seismic event at ~25 ms north of 95 m corresponds to the shallow lens of silts and clays.

in the reflection images are not due to attenuation or interference; instead, the geophysical data are imaging the changing character of the sand-clay interface from south to north.

We associate the seismic event at ~25 ms in Figure 6 with a reflection from the shallow clay lens in the north. Not only does the event correspond to the proper depth of 4 m, but the horizontal position (extending north from 90 m) also matches the extent of the shallow layer of silts and clays known from CPT exploration. This shallow event is evident in Figures 5 and 7 as well. Since the near-surface velocity is about 250 m/s, the seismic wavelength is about 1.5 m for 150-Hz data. Thus, we can resolve the shallow clay lens. Shallow refraction energy has been removed from the shot gathers prior to stack by filtering and muting, and coherent reflection energy from the shallow clay lens is seen in the first seven traces of shot gathers in the north (Figure 8). There is no interpretable event in the low-frequency GPR data that we associate with the shallow clay, although changes in the overall character of the GPR sections at 90 m north indicate changing subsurface properties. CPT data show a change in soil classification within the aquifer (Figure 2). The 1–2-m-thick lens of silts and clays in the north changes to a 3–4-m-thick silty sand in the south at roughly the same location (80–90 m north) where the change in soil classification of the aquitard boundary occurs. These changes in the soils suggest a facies transition within the aquifer and aquitard. Seismic and GPR images of the subsurface characteristics correlate with this facies change.

Interpretation of the numerous CPT data logs yields a reasonable understanding of the facies change across the GRFL. Joint interpretation of the seismic and the radar reflection data help detail the facies change above and within the aquitard. The additional detail from the geophysical data would be especially important had less CPT data been available. In addition, CPT data were collected before initial interpretation of the seismic and radar data, so there are few CPT samples around 90 m north where the aquifer/aquitard characteristics go through a transition. Choosing CPT push points after initial interpretation of the seismic and radar data would have indicated more extensive CPT collection was needed in that area.

CONCLUSIONS

We compared seismic CMP data with coincident GPR reflection profiles from the GRFL site characterization. Neither data set images a reflection from the water table, probably a result of the water saturation increasing over a thick zone. Our interpretation of seismic and GPR reflections from the aquitard boundary correlates with the CPT data, showing the aquitard deepens toward the north end of the field. Both seismic and radar images show the aquitard reflection loses coherency in the northern portion of the field. The seismic data image a shallow lens of silts and clays at 4 m depth in the north. Combined interpretation with the geotechnical data suggests a facies transition from south to north within the aquifer and aquitard. Having both seismic reflection and GPR data, in addition to CPT geotechnical data, enabled an accurate description of the subsurface at the GRFL. Acquiring good-quality seismic and ground-penetrating radar data at the same site is uncommon, and collecting good-quality seismic data from the upper 15 m is usually difficult. However, correlation with the GPR and geotechnical data at the GRFL strengthens the interpretations and conclusions determined from the seismic data alone.

ACKNOWLEDGMENTS

We thank the University of Delaware for allowing us the use of their seismic recorder, and thanks also to Prof. John Madsen for collecting the pulseEKKO data. Our thanks to Rex Morey of Applied Research Associates Inc. and Doria Kutrubes of Hager Geoscience Inc. for acquiring the low-frequency SIR data. Lt. Col. Robert Gauthier was an integral part of our field team. We gratefully acknowledge the support of our field consultants Rick Miller and Gary Olhoeft. We also thank Mark Noll from Applied Research Assoc. and the civil engineering department at Dover AFB for their support during our field work. We appreciated the suggestions from Susan Pullan and an anonymous reviewer that helped us to improve the text dramatically. This work was sponsored by the Air Force Office of Scientific Research. Any use of trade, product, or firm names

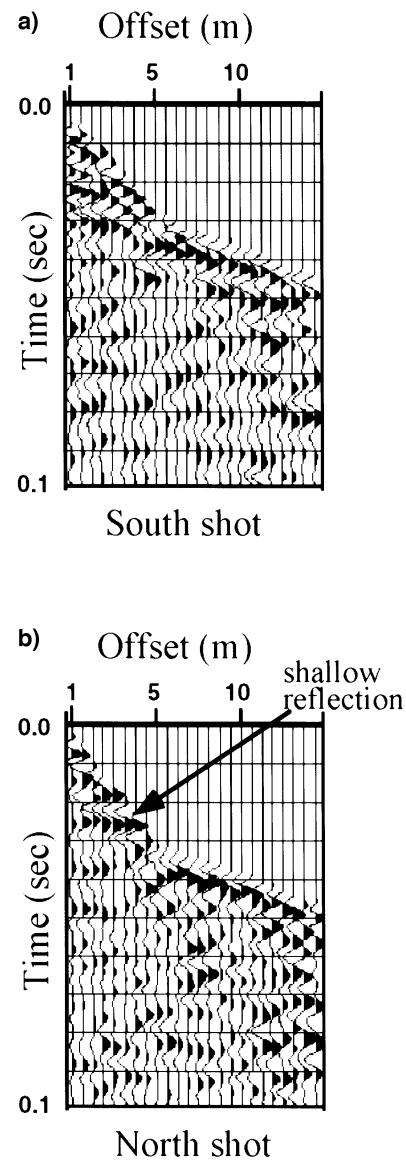

FIG. 8. Sledgehammer shot records after 80- to 300-Hz bandpass filter, f-k filter, and mute with 50-ms AGC for display: (a) shot gather from the south end of the field, (b) shot gather from the north end of the field. The reflection from the shallow lens of silts and clays in (b) is coherent across seven traces.

in this paper is for descriptive purposes only and does not imply endorsement by the Air Force Office of Scientific Research, the Air Force's Phillips Lab, or the US government.

REFERENCES

Cardimona, S., Kadinsky-Cade, K., and Clement, W., 1996a, Coincident ground penetrating radar and seismic imaging of an aquitard boundary: 66th Ann. Mtg., Soc. Expl. Geophys., Expanded Abstracts, 825–828.

Cardimona, S., Kadinsky-Cade, K., Miller, R., Pulli, J., and Turpening, W., 1996b, High-resolution seismic reflection survey at Dover AFB: A comparison of three seismic sources: 1996 Symp. Appl. Geophys. Engineer. Environ. Prob., Proceedings, 171–180.

Clement, W. P., Cardimona, S., Endres, A., and Kadinsky-Cade, K., 1997, Site characterization at the Groundwater Remediation Field Laboratory: The Leading Edge, **16**, No. 11, 1617–1621.

Miller, R. D., Pullan, S. E., Waldner, J. S., and Haeni, F. P., 1986, Field comparison of shallow seismic sources: Geophysics, **51**, 2067–2092.

Robertson, P. K., 1990, Soil classification using the cone penetrometer test: Can. Geotech. J., **27**, 151–158.